

Micro Inverter Grid Connected for PV Application Based on SEPIC Differential Inverter

Mohamed A. Ismeil^{1,2}, Hany S. Hussein^{1,3}, and M. Nasrallah^{2, □}



Abstract The problem of shading in photovoltaic systems has occupied a large part of the researchers' interests, and for this reason, the Micro-inverter (MI) is used as the solution, and the idea of manufacturing them depends on installing a small inverter with a low capacity to a small group of PV cells that agree with this rating. In addition to the interest in efficiency in the case of a connection in the standalone systems or grid electrical network. A traditional inverter was used, accompanied by a large low-frequency transformer to connect to the grid, and this led to higher costs and volume, then the idea of using different types of choppers appeared as a first stage to boost or buck the voltage, but the second stage beside the inverter stage led to higher costs, so the use of a single stage was the best solution. In addition, using MI with differential mode contributes to obtaining many advantages such as fewer passive elements (inductors and capacitors). This results in the reduced total cost and improved reliability. Among differential topologies of the AC inverters, a Single-Ended Primary-Inductor Converter (SEPIC) has been selected. This inverter was chosen because of its advantages, including the possibility of working in the boost or buck mode, and also a high-frequency pulse switching transformer can be used to act as an isolated step up/down the voltage in PV systems. The theory of differential SEPIC has been validated by PSIM software. The results will be compared with mathematical analysis.

Keywords: Micro Inverter, SEPIC, differential Inverter, PWM, Isolated inverters.

1 Introduction

Received: 23 July 2023/ Accepted: 10 September 2023

□Corresponding Author: M. Nasrallah, nasrallah_1@yahoo.com

Mohamed A. Ismeil, moalismaill@kku.edu.sa Hany S. Hussein, hany.hussein@aswu.edu.eg

1.Electrical Engineering Department, Faculty of Engineering, King Khalid University, Abha 61411, Saudi Arabia

2.Electrical Engineering Department, Faculty of Engineering, South Valley University, Qena 83523, Egypt

3.Electrical Engineering Department, Faculty of Engineering, Aswan University, Aswan 81528, Egypt

A green world without pollutants has become the strongest and most important slogan in recent times. To achieve this slogan, reducing carbon emissions is the way to reduce pollution. From this point of view, the use of sources such as wind energy and solar energy is the best solution for this.

The method of matching between these sources and the electrical grid or the different loads is one of the most important stages of the success of the electrical system.

These units of interface connection are represented in various shapes such as choppers and inverters topologies. choppers converters convert the voltage/current from a continuous form to a continuous form (DC-DC). In addition, the output voltage can be fixed or variable DC, which enables us to obtain an output voltage source that may be less than the input voltage source (step-down) or greater than the input voltage (step-up). The buck, boost, buck-boost, flyback, and Ćuk converters are examples of DC-DC converters [1-4].

Inverters topologies that convert from DC-AC come in different topologies, such as single-phase inverters or three phase inverters that are from the perspective of the number of phases or two-level Voltage Source Inverter (VSI) and multilevel inverters from the perspective of output voltage level. [5]

The current inverters are presented as one of the inverters family which has the ability to boost by using bulk inductors.

The Power Conditional Unit (PCU) is one of the famous interface units that is used with power electronic converters when it is used in non-petroleum and coal-based resources such as Photovoltaic (PV) systems or wind turbines systems. PCU includes one converter or probably more than one coupled in series or parallel according to the required target of this PCU.

2 Inverter stages types

The PCU converts the DC power into AC power for the general domestic and industrial devices in the case of PV [6]. It can be presented into two types according to the stages of converting from DC-AC:

A. Two-Stage System.

B. Single-Stage System.

2.1 Two-Stage System.

Figure 1 shows the general configuration of the two-stage system. It includes a DC-DC stage either buck or boost type. Then, the voltage at the DC link (V_i) is transformed into an AC waveform using the inversion stage. For recent decades, the Voltage Source Inverter (VSI) and the Current Source Inverter (CSI), shown in Fig. 2 and Fig. 3 respectively, are considered the most widespread inverter topologies in power electronics as a two-stage system [7].

These conventional inverters have some limitations on their operations as the following: the output voltage of VSI equals or less than the input voltage, in other words, it works only in bucking mode; Besides, the creation of dead time in the inverter switching signals is required to overcome the problem of the DC supply short-circuit. However, this dead time leads to distortion of the output voltages and, accordingly, a high rate of Total Harmonic Distortion (THD) appears, also, the value of output voltages for the traditional VSI has been reduced based on the insertion of dead time technique and the problem becomes worse when the voltage is at small levels. As a result, a large filter size must be utilized to reject the distortions in the output voltage waveform. On the other hand, CSI boosts the input voltage in DC-AC topologies; consequently, a buck stage probably will be needed if a wide range from the voltage is needed in the output of the conversion process and it can be used in AC-DC rectification topologies. Moreover, this inverter faces a big problem if the circuit is open and this can happen in the case of zero states. The main reason for this problem is the EMI noise. In addition, the two topologies (VSI, CSI) share some limitations such as:

- voltage source and current source have been used as only buck or boost, in any case, it is not used as buck/boost converter.
- The voltage source inverter has a certain function, and the current source can't be used as a voltage source.
- The performance of the two topologies is affected by the EMI noise.

From the foregoing discussion, these two-stage

systems increase the system cost and lower the overall efficiency [8]. Moreover, looking at the control side, the whole system becomes complex and requires effort to design an effective control system for both stages. In the two-stage system, there must be a capacitor called a DC-Link capacitor between the first stage (DC-DC) and the second stage (Inverter), as shown in Fig. 1, this capacitor should be chosen carefully in single phase dc-ac or ac-dc pulse width modulation converters as it suffers from double line frequency ripple (2ω ripple) because of the alternative power unbalance between the DC and AC side. For this reason, this system is not suitable for applications that are affected by double line-frequency ripple. So, using CSI eliminates the need to use a DC-Link capacitor. Single stage is suitable for achieving stable operation.

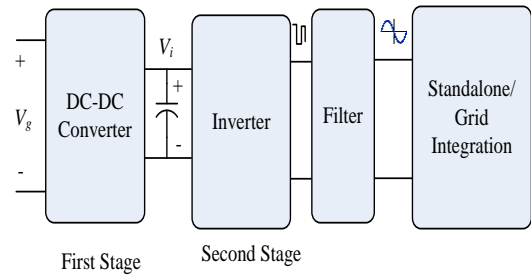


Fig. 1 General configuration of the two-stage system.

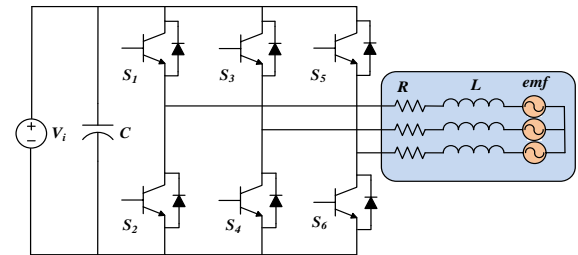


Fig. 2 Configuration of the voltage source inverter.

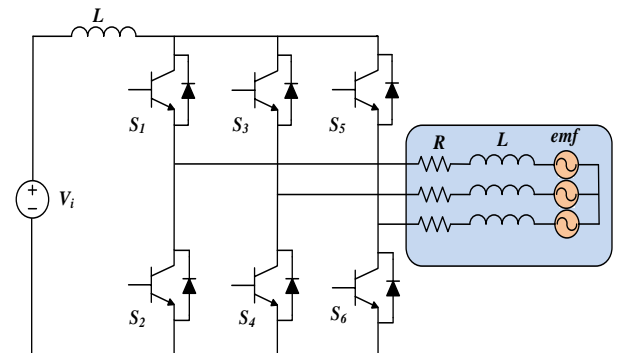


Fig. 3 Configuration of the current source inverter.

2.2 Single-Stage System.

A new family of inverters was proposed in 2002 to solve the above-mentioned barriers of the traditional VSI and CSI by Prof. Fang. Z. Peng. This family was called a

Z-source Inverter and abbreviated as ZSI [8-11] ZSI presents a single-stage inverter that combines the bucking and boosting capabilities for the input voltage within a single unit without adding extra switched devices. The basic structure of the single-stage topology is presented in Fig. 4.

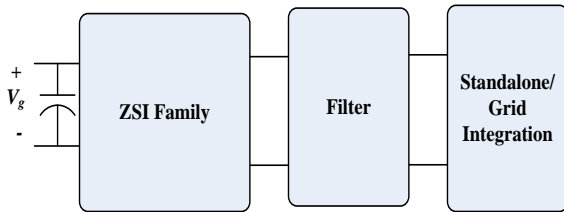


Fig. 4 Configuration of the single-stage system.

2.2.1 Z-Source Inverter Category.

This section describes the basic operation of the ZSI family; in addition to, a brief review of some of the improvements in ZSI topologies.

2.2.2 Operation of ZSI.

The basic notion of ZSI is based on utilizing the traditional PWM zero state by getting a signal in one leg for two switches at the same time (or all switches) and thus the shoot-through state has been created. The previous action is forbidden in the VSI. According to the required voltage boosting, the zero state can appear as the shoot-through state or part of it, and the rest traditional zero state when all upper switches are turned on, or all lower switches are turned on. The construction of the basic topology has an X-shape with two inductors and two capacitors as linear storage elements, and one diode in the front connection; these elements are cascaded by the conventional inversion stage (either single-phase or three-phase) as depicted in Fig. 5. The Z-Source network tank can be used also second order filter for the fluctuation in the DC voltage source. The existence of the input inductors and capacitors in the Z-Source network makes the problem of the VSI inverter an advantage, as it allows the switches in the same leg to work at the same moment, allowing the coils to be charged, and in this case, is called shoot-through.

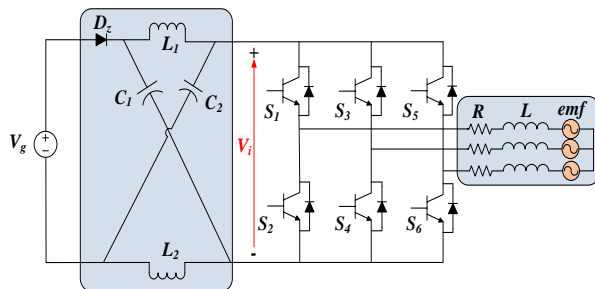


Fig. 5 Configuration of the basic Z- Source Inverter.

The normal theory of ZSI operation can be allocated into two modes according to the state of its switches as :

- a. Non shoot-through case contains eight states, six active states in which the diode is being in forward biasing; the load is tied into the DC source, and the energy starts flowing through it. Moreover, the extra two states are zero state (null case) in which the diode is turned off and there is no power transferred to the load.
- b. Shoot-through case where all the inverter switches have been turned on at the same time and the inductor is charging, while the capacitor is discharging.

By applying the voltage equilibrium and charge balance for the capacitor and inductor, respectively, of the converter LC network in the above cases; the boost factor (B) of ZSI that presents the relation between the input DC voltage (V_g) and the pulsated DC link voltage (V_i) can be formulated as:

$$B = \frac{V_i}{V_g} = \frac{1}{1 - 2.D} \quad (1)$$

where B is the boost factor, V_g is the input voltage, V_i is the pulsated DC link voltage, D is the shoot-through duty cycle.

2.2.3 Brief Review on ZSI Topologies.

Insufficient boost factor, higher voltage stresses across the capacitors, inrush current, and discontinuous input current are the main drawbacks of the basic topology of ZSI. Many improvements have been made to the fundamental topology of ZSI to get over these weaknesses. These improvements can be classified as:

- ✓ Rearrangement of the basic LC Z-network construction. This develops the ZSI features such as making the drawn current from the source to be continuous and improving the Electro-Magnetic Interference (EMI). Examples of this class are (quasi Z-Source Inverters (qZSI) and Embedded Z-Source Inverters (EZSI))[12-13].
- ✓ Cascaded connection of similar LC qZ-networks. This upgrades the features to have continuous input current, reduces the effect of Electromagnetic Interference (EMI), and partially solves the problem of dependence between voltage gain (G) and modulation index (M). An improved Example of this class is the Cascaded quasi

Z-Source Inverter (CqZSI) [14].

- ✓ Using the Switched-Inductor cell instead of the two main inductors in ZSI network. This improves the problem of dependence between voltage gain (G) and modulation index (M). Examples of this class are Switched-Inductor ZSI (SL-ZSI) in [15-16].
- ✓ Series connection of LC impedance with the inverter is resulting in reducing the stress on the capacitor and reducing inrush current. Examples of this class are improved/series Z-Source Inverter [17-19].
- ✓ Recently The topology of quasi-Z-Source Inverter has been derived from Z-Source inverter (ZSI) which has been presented in Fig. 6 [20-21] and when compared to the basic ZSI circuit, qZSI has clear advantages besides all ZSI advantages that can be summarized as:
- ✓ It works in Continuous Conduction Mode (CCM), so, Continuous input current is achieved, and this helps to extend the life of the equipment used, increase the efficiency (by reducing dissipation), and achieve lower differential mode noise.
- ✓ Less stress on the passive elements such as the capacitor C2, which reduces the total cost of the device and also contributes to reducing the size of the device.

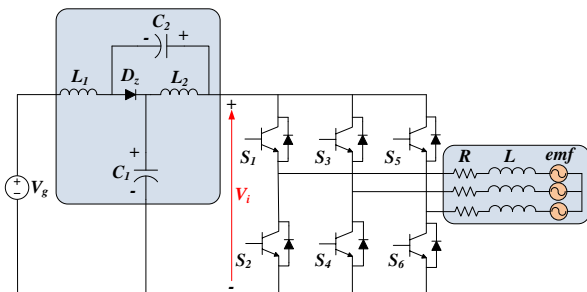


Fig. 6 Configuration of quasi ZSI.

3 Microinverter

The easy way to connect inverters in a home solar electric system connected to the grid is to use a single inverter for each module. This connection leads to other important advantages, including overcoming the problem of shadows. From this standpoint came the importance of using the microinverter. For this reason, recent research has focused on the development of the microinverter, and despite the increased cost of using this inverter, it has

many advantages, including: [22-25]

- ❖ Improve the maximum power for the PV arrays, this comes with the use of a Maximum Power Point Tracker (MPPT) on each module.
- ❖ Solving the problem of shading. Expected to increase capacity. Laboratory studies have shown that shading of up to 9% of the solar system connected to a central inverter leads to a system-wide reduction in energy production of up to 54%.
- ❖ Due to the increasing energy demand, it aligns with the future vision of expanding the station's capacity.
- ❖ Direct conversion from direct current/voltage (DC) to alternating current /voltage (AC) at the array site.
- ❖ Not noisy as it creates less heat, so, there is no need for cooling.

Micro Inverter (MI) is a small inverter in the form of a plug-and-play device compatible with photovoltaic systems, where it converges the DC voltage to AC voltage for a single photovoltaic module. Hence, it is called a PV inverter. In the market, there is a 2kw rating as shown in Fig. 7 Because it is operated at this lower PowerPoint, The installation of MI is very simple because there is no need for a large component of wiring and soldering. MI is a promising inverter, and it has presented in different types such as the IQ7 Series micro-inverter series [26].



Fig. 7 2000W Solar Micro Inverter [26].

The main advantage of MI is that very efficient in shading weather and it has a large overall efficiency. as shown in the illustration Fig. 8. Under using MI, the panel output quality is the main issue. If the same panels have the same production the studies prove that the rated output can vary by as much as 10% or more. This can happen only by using MI, not string configuration. The maximum power in MI can be achieved. In addition, the reparation of MI can be done or change easily when the condition changes or the power demands change from each cell.

Not only maintenance is easy in MI but also monitoring. Because the power output of their units should be presented or monitored [27].

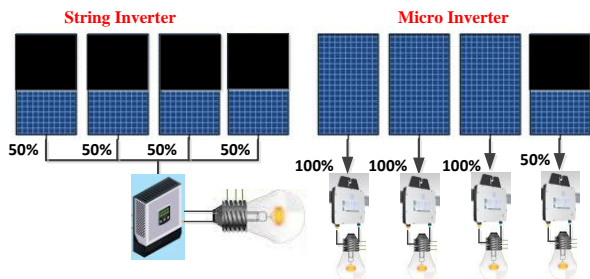


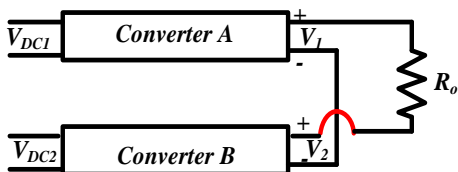
Fig. 8 Configuration of string and Micro inverter under a shadow.

The main disadvantage of MI use in PV systems is the high cost. At the beginning of 2022, the cost of a microinverter was recorded at \$0.36 per watt, whereas the cost for a central inverter was recorded at \$0.13 per watt [28].

The number of MI modules produced takes into consideration the economic force of manufacturers to push the cost to decrease. A single model has been produced which may be over or lower than the specifically matched panel [29].

4 Differential Inverters.

The impedance inverters have been presented as a single stage with the ability to boost without using the low-frequency transformer, Despite the advantages offered by this inverter, it faces many problems, including high voltage stress of semiconductor gadgets, and low boosting ability. Differential inverters have been presented to improve single-stage inverters because of their advantages such as low cost, large boosting, and low passive component counts. The sinusoidal modulation has been used to drive two buck-boost stages to create the shifted AC voltage, then the shifting can be removed by differential way across the output DC-DC converters. The injected signal shifted by 180o [30]. as shown in Fig. 9.



a)

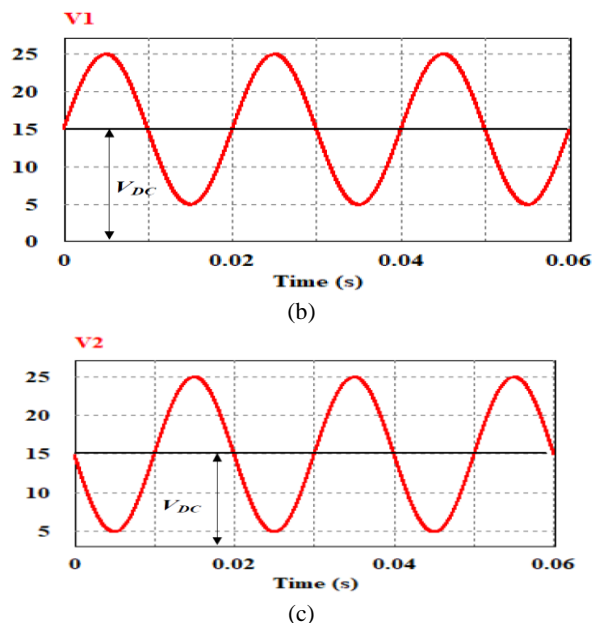


Fig. 9 Conception structure of single-phase differential inverter.

The control methodology of this inverter is to use two sinusoidal waves by two 180° phase shifts. The load is supplied from the differential connection of the two buck-boost converters hence the DC offsets from the output voltage can be removed and the total system can feed larger or lower AC voltage than the DC input voltage. This topology used large capacitance across the output [30].

The basic idea of constructing a three-phase AC power supply from the previous model is to use three buck-boost as shown in Figure 10, noting that buck-boost A is fed by a zero-phase shift PWM wave (Da), and the buck-boost B is fed by a 240o phase shift PWM wave (Db). and the buck-boost C is fed by a 120o phase shift PWM wave (Dc). The outputs are connected differentially across the AC loads or grid-connected.

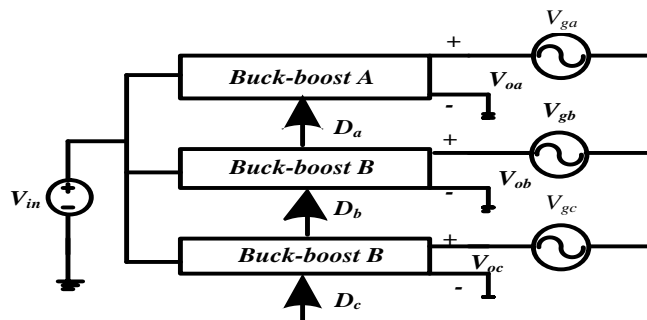


Fig. 10 Conception structure of three phase differential inverter.

5 Single-Ended Primary-Inductor Converter (SEPIC).

There are a lot of buck-boost converters. Among these converters, the Single-Ended Primary-Inductor Converter (SEPIC) converter has the lowest losses and the best voltage regulation.

The SEPIC converter consists of active switches components such as two active power switches (MOSFET), and four passive components such as two inductors (L_1 , L_2) and two capacitors (C_1 , C_2). The capacitor C_1 , is located between the two inductors L_1 and L_2 , [31]. Moreover, the inductor L_2 in Fig. 11 can be replaced by an isolated transformer which leads to an increase in the voltage boost ability. SEPIC can work in boosting and bucking modes. In addition, the converter shares the same reference between input and output, and it maintains the same polarity.

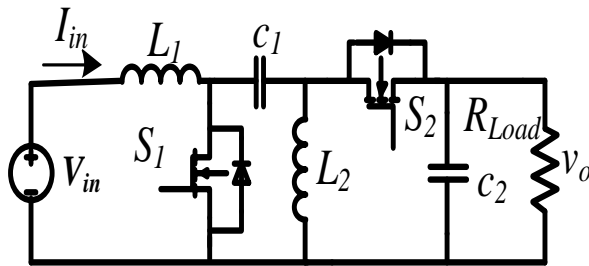


Fig. 11 Single-Ended Primary-Inductor Converter (SEPIC).

The main assumption in SEPIC analysis is that the SEPIC works in Common Conduction Mode (CCM). The two switches work in complements, so it has two modes.

- **Mode 1 (switch turn on).**

In this mode the switch S_1 is firing on, the inductor L_1 is connected in series with the input voltage V_{in} , also the capacitor C_1 is connected directly to L_2 , in addition, the load capacitor C_1 is connected directly to the output load. To supplement the explanation of the work of the circuit, the inductor L_1 charge from the DC input voltage source (V_{in}) is shown in Fig. 12. The second inductor L_2 charges from the capacitor C_1 . In this mode, there is no energy transfer from the input to the load capacitor C_2 .

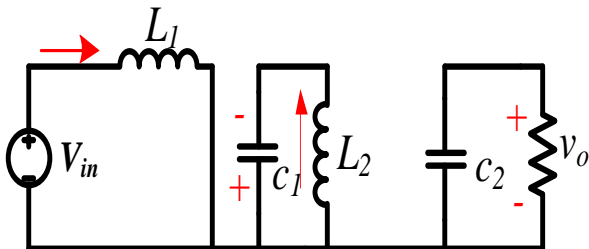


Fig. 12 Mode 1 switch on.

- **Mode 2 (switch turn off).**

In the second mode, the switch is turned off, and the

input voltage V_{in} is connected in series with the two passive elements (L_1 and C_1) and delivers the power to both inductor L_2 and capacitor load. Both two inductors are delivering the current to the load and capacitor load as shown in Fig. 13.

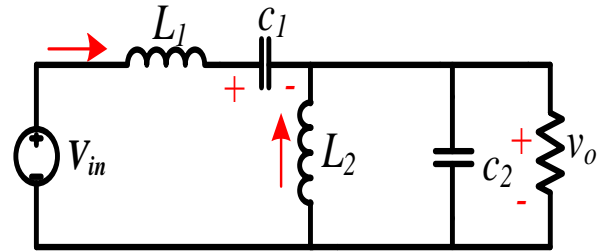


Fig. 13 Mode 2 switch off.

In both modes, the input current appeared in the Continuous Conduction Mode (CCM). The main objective in designing inverters was to avoid the use of line frequency transformers. Switched Mode Power Supplies (SMPS) have been presented to solve this problem such as SEPIC. In addition, a high pulse switching transformer can be integrated into SEPIC as shown in Fig. 14. Moreover, the presence of an interleaving pass of current enables easy parallel connection and this is a trend for PV application to the same point of common coupling (PCC). The C_{in} is used as a DC-Link capacitor whereas, in a Switching Power Supply (SPS), the place of the DC link capacitor is after the rectification unit and before the inverter switches in parallel with the rectification unit and input of the inverter as shown in Fig. 14.

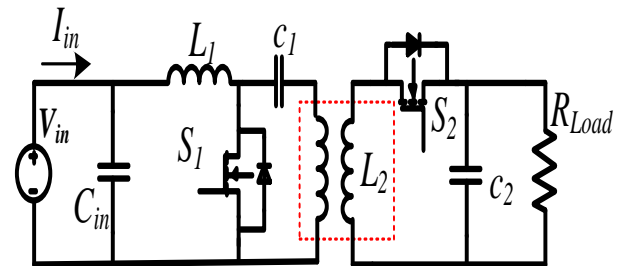


Fig. 14 Single-Ended Primary-Inductor Converter (SEPIC) with high frequency transformer.

6 Three phase Coupled Inductor SEPIC Converter.

the Single-Ended Primary-Inductor Converter (SEPIC) converter will be presented as a single-stage-three phase deferential topology inverter as shown in Fig. 15.

The system consists of three modular SEPIC converters each modular has two switches, two capacitors, one high frequency transformer, one inductor, and input voltage connected via a grid network or different loads

across the filters for three phase. The proposed inverter is a good solution for PV applications where the peak AC output voltage can be controlled when the input DC is low or high based on MPPT operation and for providing easy paralleling at the PCC.

The system converts the DC input to AC across three SEPIC modules and is connected to the grid across the filters. A detailed analysis has been presented by [32]. The grid phase voltages are represented as:

$$\begin{cases} v_a = V_m \sin(\omega t) \\ v_a = V_m \sin(\omega t - 120^\circ) \\ v_a = V_m \sin(\omega t + 120^\circ) \end{cases} \quad (12)$$

The basic idea to produce the AC voltage is that the system is connected in a differential way. The system will be driven by quazi sinusoidal PWM with phase shift 120o. The differential connection will remove DC components. The DC offset for each DC-DC converter VC1B over the total output voltage can be presented as:

$$\begin{cases} v_{C1B}(t) = -h_a V_{in} \\ h_a = H_{dc} + H_{ac} \sin(\omega t + \theta) \\ v_{C1B}(t) = -[V_{dc} + V_m \sin(\omega t + \theta)] \end{cases} \quad (13)$$

where:

θ is the voltage phase-shift, h is the transfer ratio, the DC and AC voltages ratio can be represented as H_{dc} , and H_{ac} , V_{dc} is the shifted DC component of the buck-boost, and V_m is the peak value of the output AC component.

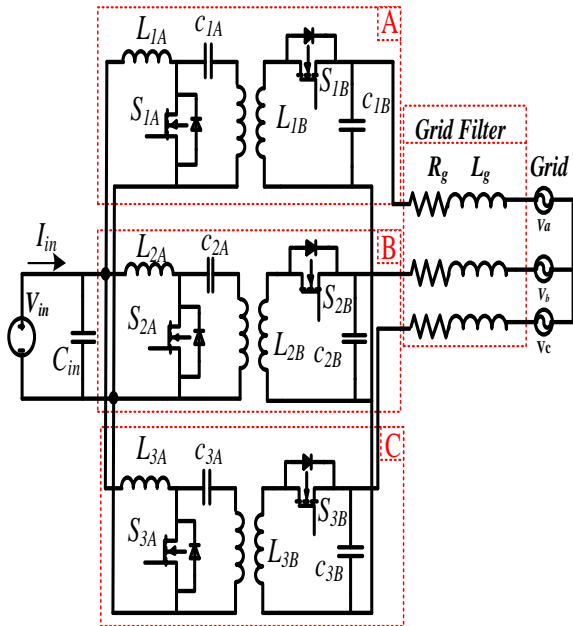


Fig. 15 Conception structure of a three-phase differential inverter.

6.1 SEPIC analysis.

By applying, this on the b and c phases the voltage, V_{C2B} , V_{C3B} , can be presented as:

$$\begin{cases} v_{C2B}(t) = -h_b V_{in} \\ h_b = H_{dc} + H_{ac} \sin(\omega t + \theta - 120^\circ) \\ v_{C2B}(t) = -[V_{dc} + V_m \sin(\omega t + \theta - 120^\circ)] \end{cases} \quad (14)$$

and,

$$\begin{cases} v_{C3B}(t) = -h_c V_{in} \\ h_c = H_{dc} + H_{ac} \sin(\omega t + \theta + 120^\circ) \\ v_{C3B}(t) = -[V_{dc} + V_m \sin(\omega t + \theta + 120^\circ)] \end{cases} \quad (15)$$

From (2) the voltage conversion ratio is :

$$h_a = \frac{v_{C1B}(t)}{V_{in}} \quad (16)$$

So, the sinusoidal duty ratio D_a can be presented as:

$$D_a = \frac{h_a}{1+h_a} = \frac{M(\sin(\omega t + \theta) + 1)}{M(\sin(\omega t + \theta) + 1) + 1} \quad (17)$$

where ,

$$M = \frac{v_m}{V_{in}}$$

The DC offset cancellation can't be achieved with an unbalanced energy operation of the three phases, hence pure AC sinusoidal voltage and current have appeared. Assuming that the switching period T_s is very small which led to a linear energy transfer; the relation of the ripple ΔI_{L1} and ΔI_{L2} with L_1 and L_2 when the switch S_1 is on can be described as [32] :

$$\left. \begin{aligned} V_{in} &= L_1 \frac{\Delta I_{L1}}{\Delta t} \\ L_1 &= \frac{V_{in} D}{\Delta I_{L1} f_s} \\ V_o &= \frac{V_{in} D}{\Delta I_{L1} f_s} \\ L_2 &= \frac{V_o D}{\Delta I_{L2} f_s} \end{aligned} \right\} \quad (18)$$

To obtain the equation concerning C_1 the assumption of neglecting the small change in the inductor current I_{L2} is valid and the ripple of capacitor voltage C_1 can be calculated when S_2 is on as:

$$\left. \begin{aligned} I_{L2} &= C_1 \frac{\Delta V_{C1}}{\Delta t} \\ C_1 &= \frac{(1-D)}{\Delta V_{C1} f} I_{L2} \end{aligned} \right\} \quad (19)$$

where, I_{L2} is the average output current over the sampling period T_s .

From the previous equation, the values of C_1 and $L_{1,2}$ can be chosen to be equal to or greater than a minimum

value that comes from equations (18), (19).

7 Control of Power Converters.

The control design is an essential stage in any system; it has good attention in recent years. For the key research area of power electronics converters; several control methods have been developed; some of the most popular utilized ones are categorized in Fig. 16 as mentioned in [33]. Hysteresis control is a nonlinear type that determines the switching states by comparing the feedback values from the controlled items with their set points, within a certain band of the error. It is generally used for simple purposes such as the current control of the converters. Besides that, it begins to embed with complex methods such as Direct Torque Control (DTC) [34] and Direct Power Control (DPC) [35]. The nonlinearity of the system and tolerable error width lead the system to operate at the variable switching frequency, which can produce resonance difficulties [33] To avoid these limitations, a bulky and expensive filter is used in the system design. On the other hand, the linear control that is established on the existence of PWM control schemes is another most common type especially Proportional-Integral (PI). The linear control with the modulation stage often requires additional transformation such as Park transformation from three-phase quantities (abc) into two DC quantities (dq).

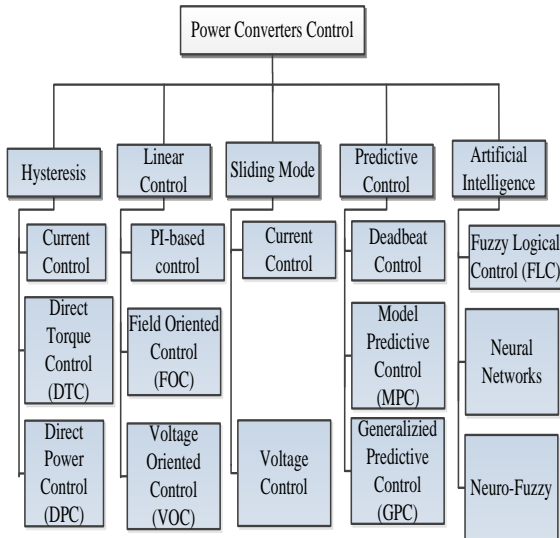


Fig. 16 Classification of power converters control schemes [33].

8 Block Diagram of SEPIC Control.

8.1 PID controller design.

Fig. 17 represents the full control block diagram, the

methodology of the control depends on the transfer of the three output currents into the D-Q platform. The reference Idref is compared with Id across the addition block and the output error is converted to a control signal across the PI compensation transfer function.

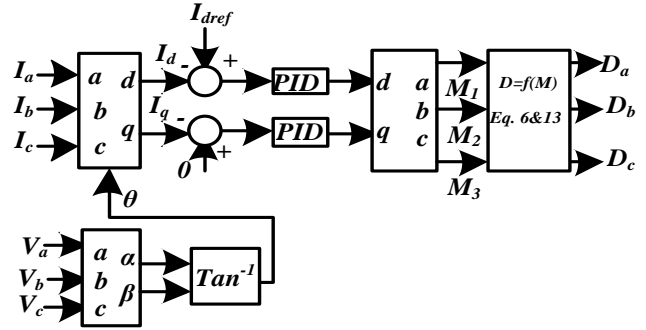


Fig. 17 Block diagram of feedback control.

The main reason for the widely employed PID is that this technique is very understandable and strongly effective. Another important point for PID is that the effects of differentiation and integration are understood and don't need to be analyzed in all systems.

The compensation transfer function with PID can be obtained by manually tuning or by software tuning such as MATLAB tuning.

The effect of the PID parameter on the closed-loop transfer function will be discussed based on the dynamics load.

The transfer function of a PID controller is found by taking the Laplace transform of Equation (20).

$$K_p + \frac{K_i}{s} + K_d s \quad (20)$$

Where: K_p is the proportional gain, K_i is integral gain, and K_d is derivative gain.

The proportional gain (K_p) is used to eliminate the oscillation associated with on-off controllers. In other words, the effect of K_p is strongly affects the steady-state error.

The addition of a derivative term to the controller (K_d) is used to speed up the anticipation of error. although it does not affect the steady-state error and it is used to add damping to the system. Also, an integral term to the controller (K_i) can be used to decrease the steady-state error. However, increasing K_i it makes the system oscillatory.

The automatic tuning of these parameters can be achieved by optimization methods such as PSO.

9 Simulation Results.

PSIM software has been used to validate the analysis and all theories. Parameters for the SEPIC topology are listed in Table 1.

In this paper, the DC source is used as input voltage instead of the PV source as the output of the PV cell is DC voltage and the main contribution is to use the SEPIC inverter as an interface between the DC source and grid network. In addition, the connection between the SEPIC and three phase grid (V_a, V_b, V_c) is achieved across the inductor filter L_g . Also, the coupling inductor C_{in} can be used between the DC source and the SEPIC inverter. The High-Frequency transformer (HF) is used as an isolation transformer and for boosting the voltage across the turns ratio of the HF transformer. Each module has two switches (S_{1A}, S_{1B}), two inductors (L_{1A}, L_{1B}), and two capacitors (C_{1A}, C_{1B}).

Table 1 Parameters of SEPIC Inverter.

Parameters	value	Parameters	value
V_{in}	120V	$C_{1,2,3(A)}$	10 μ F
C_{in}	400 μ F	$C_{1,2,3(B)}$	10 μ F
f	50kHz	L_g	4mH
$L_{1,2,3(A)}$	400 μ H	Internal resistance R_g	100m Ω
$L_{1,2,3(B)}$ Or mutual for transformer	350 μ H	Phase Grid voltage V_a	80sin(ωt)
$N1/N2$	1		

9.1 Sinusoidal PWM for SEPIC Inverter.

The duty ratios of the SEPIC inverter D_a, D_b, D_c are calculated from h_a, h_b and h_c in equation (13, 14, 15, 17) the Sinusoidal D_a varies from 0 to 0.6667 as shown in Fig. 18.

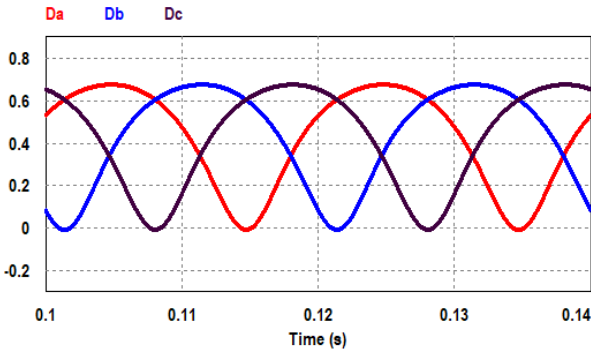


Fig. 18 Sinusoidal duty ratios of the SEPIC inverter D_a, D_b, D_c .

The firing switching for each switch is shown in Fig. 19. After creating ($D_{a,b,c}$) each one has been compared with a triangle wave 50kHz. The output of each goes directly to the main switches (S_{1A}, S_{2A}, S_{3A}) where the complement goes to the switches (switches (S_{1B}, S_{2B}, S_{3B})).

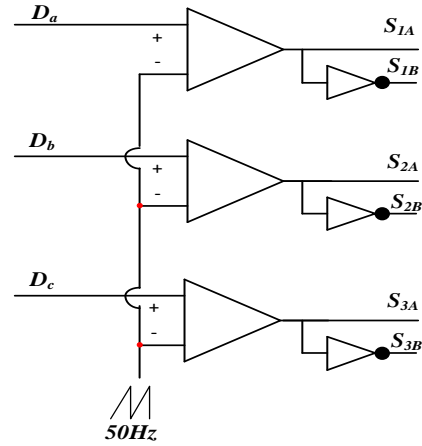


Fig. 19 Switching firing creating.

It is important to discuss the stress for the SEPIC inverter so Fig. 20 shows the capacitor voltage of the capacitor VC_{1A} and the capacitor voltage of the capacitor VC_{1B} . It is worth mentioning that the voltage VC_{1B} is an alternative voltage with a DC offset voltage equal to 84V and it has a high ripple value which equals 168V. The DC offset will be removed according to the differential connection, however, the voltage VC_{1A} is an almost straight line and its average value is 120V.

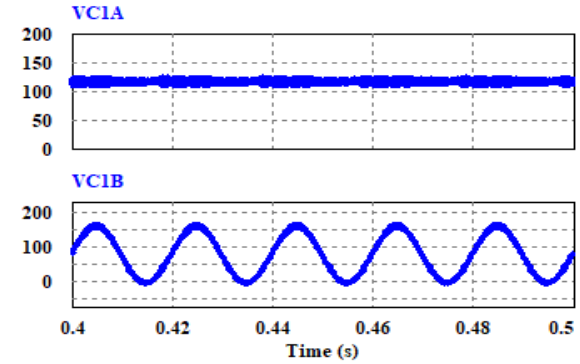


Fig. 20 Capacitor voltage VC_{1A}, VC_{1B} .

The inductor currents for L_{1A} and L_{1B} have been presented in Fig. 21. It is worth mentioning that both currents have low-frequency ripples on the main wave of the inductor current. The Zoom of the current wave shows that the inductor has to charge mode and discharging mode.

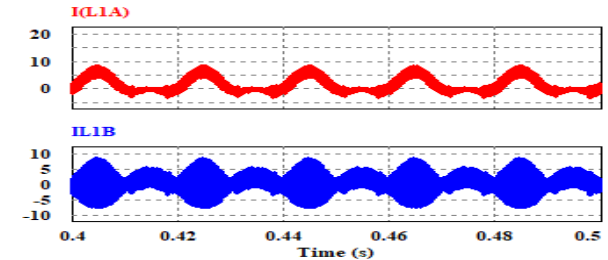


Fig. 21 Inductor Currents for L_{1A}, L_{1B} .

Fig. 22 shows the switch's current across switch S1A and S1B . The two modes of the switch operation are shown in Fig. 22 where the switch is on and in the second mode the switch is off.

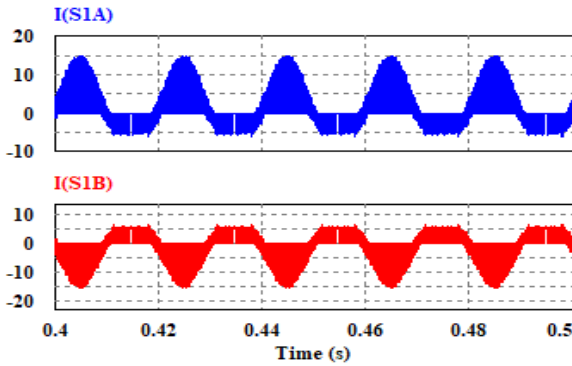


Fig. 22 switches Currents for S1A, S1B.

The sinusoidal signals in the ABC frame are converter to a constant value in the dq0 reference frame. The d-vector has a constant value where q- the vector equals zero at balanced currents.

Fig 23 shows the D-Q currents which indicate that at a balanced current, the value of Iq equals zero.

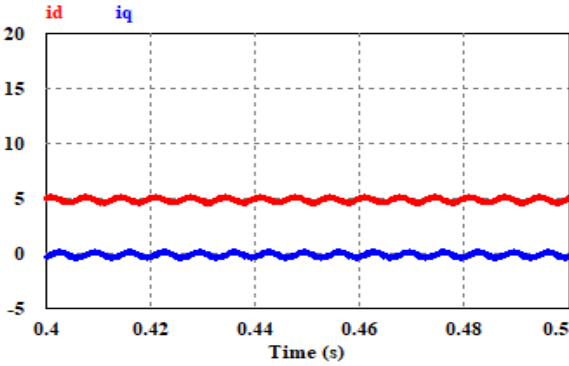


Fig. 23 Id and Iq current reference frame.

The input DC current and its 50 kHz ripple are shown in Fig. 24. The current is working under Continuous Conduction Mode (CCM) as shown in the zoom shape in Fig. 24. The CCM is an optimal solution for the constant load under low input noise and low output ripple. However, the Discontinuous Conduction Mode (DCM) presents higher efficiency than CCM, due to reverse recovery loss on the diode and the MOSFET.

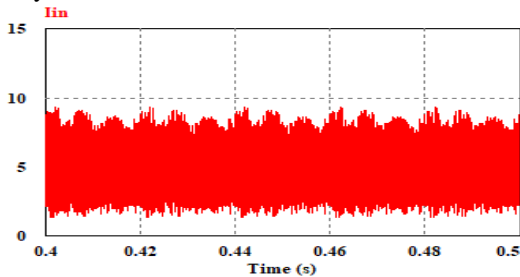


Fig. 24 Input current.

The phase voltage is shown in Fig. 25 with the peak voltage being 80 V. A typical grid synchronization strategy is achieved by generating the angle theta and detecting it as shown in Fig. 25 and it is used in dq frame transformation.

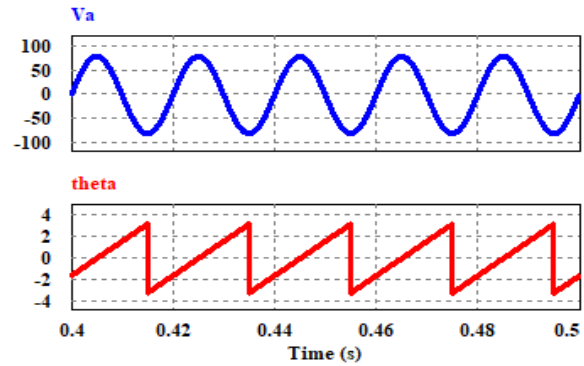


Fig. 25 phase detector for grid voltage.

9.2 PID Compensation Transfer Function for SEPIC Inverter Under dynamic load change.

For a good dynamic and fast response, the compensation transfer function consists of PI flowed with first-order s-domain transfer function

In this paper, the parameters are chosen as: at maximum $D=0.6667$:

Proportional-integral (PI) controller $(G(s) = k \frac{sT+1}{sT})$ (gain 13m, Time Constant 2m)

s-domain transfer function block $(G(s) = k \frac{B_1s_1+B_0}{A_1s_1+A_0})$ (order n=1 , k= 1, B1=0, Bo=1, A1= 0.00077 , Ao=1 The values of this controller are chosen to be small so as not to interrupt the main PI loop.

The direct current Id_ref has been changed to step up from 5 A to 10A the response of the system under dynamic is presented in Fig. 26 which indicates that the actual value of Id follows the reference value Id_ref.

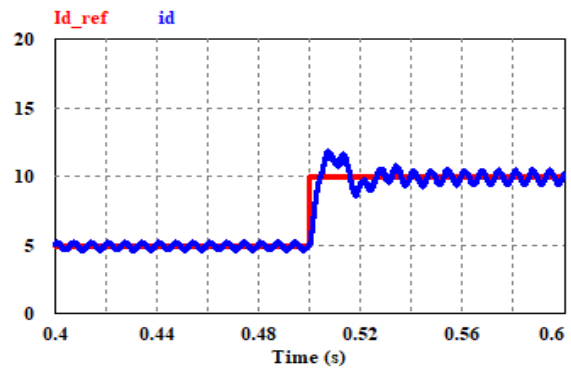


Fig.26 Actual value of Id and reference value Id_ref.

The output load currents for the three phase current

are shown in Fig. 27. The current is changed during the dynamic load at 0.5s.

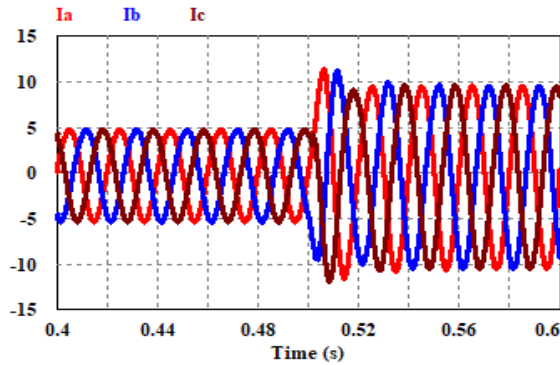


Fig. 27 Three phase output current.

The grid voltage has been shown in Fig. 28 which each phase has a maximum voltage of 80V with an RMS value equal to 100V. In addition, the grid voltage is stable under dynamic response at 0.5s.

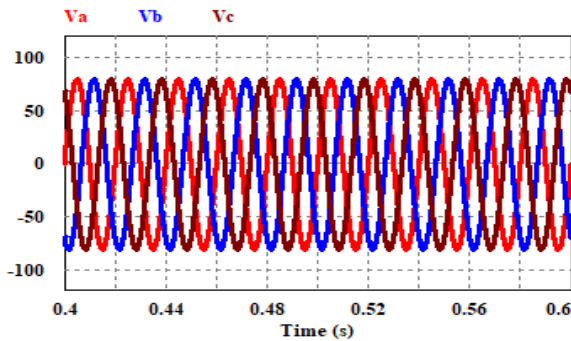


Fig. 28 the three phase grid voltage V_a , V_b , V_c .

The important goal for any utility company is to work under a unity power factor. Thus if the power factor is less than one the utility grid delivers reactive power and for the same power, the grid gives more current to maintain the apparent power, so more power losses appear, and large capacity equipment is needed. In many countries, there is a penalty if the power factor for an industrial facility moves from the value one. Each industrial facility has a unit called power factor correction that consists of a large number of capacitors. The system works under the unity power factor as shown in Fig. 29.

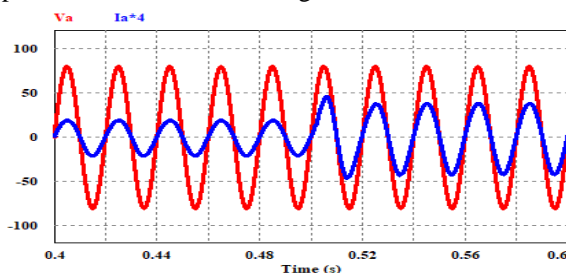


Fig. 29 voltage and current for the same voltage.

10 Conclusion.

Differential inverter based on SEPIC introduces several advantages when it is used for PV applications such as Continuous Conduction Mode (CCM) operation, and large buck-boost mode operation using a high-frequency transformer. In other words, the CCM led to generating direct MPPT techniques and allowed all designers to use paralleling DC-AC inverters under the same condition as a viable topology for PV applications.

In this paper, the Microinverters are attached to connect individual solar panels. string inverters for each module have their own Maximum Power Point Tracker (MPPT) which means that under the shading problem, the panels facing the shading only decrease the power delivered where the other panels work normally which can reach 50% saving of power.

In this paper, a three phase differential inverter based on the SEPIC inverter has been presented and analyzed with detailed analysis. All analysis is verified by PSIM software. The control has been verified under dynamic response. The results prove that the system is stable under dynamic response and the actual value of the current follows the reference values. The system under prosed control succeeded in working on the unity power factor.

References

- [1] Saadat, S. A., Ghamari, S. M., & Mollaei, H. (2022). Adaptive backstepping controller design on Buck converter with a novel improved identification method. *IET Control Theory & Applications*, 16(5), 485-495.
- [2] Ahmed, H. Y., Abdel-Rahim, O., & Ali, Z. M. (2022). New High-Gain Transformerless DC/DC Boost Converter System. *Electronics*, 11(5), 734.
- [3] Akay, C., YILDIRIM, O., CALIK, H., OZOGLU, Y., & YILMAZ, S. (2022). Flyback Converter Design for Polymer Based Organic Panels. *International Journal of Renewable Energy Research (IJRER)*, 12(4), 2092-2100.
- [4] Heidari, R., Adib, E., Jeong, K. I., & Ahn, J. W. (2022). Soft-switched Boost-cuk-type High Step-up Converter for Grid-tied with Half-bridge Inverter. *IEEE Journal of Emerging and Selected Topics in Power Electronics*.
- [5] Assunção, G. D. O., & Barbi, I. (2022). Method for deriving transformerless common-ground voltage source inverter topologies. *IEEE Transactions on Power Electronics*, 37(9), 10821-10832.
- [6] Erickson R. W., and Maksimovic D. (2007) "Fundamentals of Power Electronics," Springer Science & Business Media, 2nd Edition, Chapter 1.
- [7] Dai, H., Torres, R. A., Lee, W., Jahns, T. M., & Sarlioglu, B. (2020, October). High-frequency evaluation of two-level voltage-source and current-source inverters with different output cables. In *2020 IEEE Energy Conversion Congress and Exposition (ECCE)* (pp. 2403-2410). IEEE.
- [8] Siwakoti Y. P., Peng F. Z., Blaabjerg F., Loh P. C., and Town G. E.,(2015) "Impedance Source Networks for Electric Power

- Conversion Part I: A Topological Review,” IEEE Transaction on Power Electronics, vol. 30, no. 2.
- [9] Peng, F. Z., (2003) ‘Z-Source Inverter,’ IEEE Transaction on Industry Applications, vol. 39, no. 2, pp. 504-510.
- [10] Siwakoti Y. P., Peng F. Z., Blaabjerge F., Loh P. C., Town G. E., and Yang S.,(2015) ‘Impedance-Source Networks for Electric Power Conversion Part II: Review of Control and Modulation Techniques,” IEEE Transaction on Power Electronics, vol. 30, no. 4, pp. 1887-1906.
- [11] Ahmadi, A., Asadi, Y., Amani, A. M., Jalili, M., & Yu, X. (2022). Resilient Model Predictive Adaptive Control of Networked Z-source Inverters using GMDH. IEEE Transactions on Smart Grid, 13(5), 3723-3734.
- [12] de Oliveira-Assis, L., Soares-Ramos, E. P., Sarrias-Mena, R., García-Triviño, P., González-Rivera, E., Sánchez-Sainz, H., ... & Fernández-Ramírez, L. M. (2022). Simplified model of battery energy-stored quasi-Z-source inverter-based photovoltaic power plant with Twofold energy management system. Energy, 244, 122563.
- [13] Huynh, A. T., Ho, A. V., & Chun, T. W. (2022). Active Switched-Capacitor Embedded Quasi-Z-Source Inverter and PWM Methods for High Boost Capability and Switching Loss Reduction. IEEE Access, 10, 119301-119313.
- [14] Li, Z., Xi, W., Cao, Y., & Pu, S. (2023, May). A Dimensional Reduction Optimization Strategy for Line Voltage cascade Quasi-Z-Source Inverter Based on GRA-PCA-PSO. In Journal of Physics: Conference Series (Vol. 2488, No. 1, p. 012053). IOP Publishing.
- [15] Das, S. S., & Panda, A. (2022). Extended boost active switch-controlled switched inductor-based Z-source inverter. International Journal of Circuit Theory and Applications, 50(2), 683-705.
- [16] Ismeil M. A., Kouzou A., Kennel R., Abu-Arub H., and Orabi M.(2012)’, “A New Switched-Inductor Quasi-Z-Source Inverter Topology,” in proc. 15th International Power Electronics and Motion Control Conference (EPE-PEMC), pp. DS3d2-1- DS3d2-6.
- [17] Saranya, D., Irshath, M., Imthiyas, S., & Vallarasu, S. (2022, October). Improved series z-source multi level inverter using control techniques for grid tied PV system. In AIP Conference Proceedings (Vol. 2455, No. 1, p. 040008). AIP Publishing LLC.
- [18] Gan, S., & Shi, W. (2022). An improved Z-source inverter with high voltage boost ability. Electrical Engineering, 104(2), 869-881.
- [19] Ismeil M. A., Kouzou A., Kennel R., Ibrahim A. A. , Orabi M., and M. E. Ahmed, (2012). ‘Improved Switched Inductor (SL) Z-source,’ International Review on Modelling and Simulation Journal (IREMOS), vol. 5, no. 2, pp. 771-778.
- [20] Zhu, X., Zhang, B., & Qiu, D. (2019). A high boost active switched quasi-Z-source inverter with low input current ripple. IEEE Transactions on Industrial Informatics, 15(9), 5341-5354.
- [21] Ismeil, M. A., Bakeer, A., & Orabi, M. (2019). Implementation Quasi Z-source inverter for PV applications based on finite control set-model predictive control. International Journal of Renewable Energy Research (IJRER), 9(3), 1462-1471.
- [22] Yaqoob, S. J., Obed, A., Zubo, R., Al-Yasir, Y. I., Fadhel, H., Mokryani, G., & Abd-Alhameed, R. A. (2021). Flyback photovoltaic micro-inverter with a low cost and simple digital-analog control scheme. Energies, 14(14), 4239.
- [23] Sivaraman, P., & Sharmeela, C. (2020). Solar micro-inverter. In Handbook of research on recent developments in electrical and mechanical engineering (pp. 283-303). IGI Global.
- [24] Guo, L., Wang, Y., Kang, R., Wang, R., Li, Y., & Yang, S. (2022). Energy yield optimization for micro-inverter photovoltaic systems with spare parts inventory. Sustainable Energy Technologies and Assessments, 53, 102729.
- [25] Saeedinia, S., Shamsi-Nejad, M. A., & Eliasi, H. (2022). A two-stage grid-connected single-phase SEPIC-based micro-inverter with high efficiency and long lifetime for photovoltaic systems application. Iranian Journal of Electrical and Electronic Engineering, 18(2), 2355.
- [26] Enphase, IQ 7, IQ 7+, and IQ 7X Microinverters, 2018 < <https://static1.squarespace.com/static/5354537ce4b0e65f5c20d562/t/5d54a458659dd900016bac5b/1565828186641/Enphase+IQ7+IQ7%2B+IQ7X-data-sheet-INTL-AU.pdf>>
- [27] maxsunshine, 2022, ‘Monitoring System’ <<https://enecsys-monitoring.com/>>
- [28] Ramasamy, V., Zuboy, J., O’Shaughnessy, E., Feldman, D., Desai, J., Woodhouse, M., ... & Margolis, R. (2022). US Solar Photovoltaic System and Energy Storage Cost Benchmarks, With Minimum Sustainable Price Analysis: Q1 2022 (No. NREL/TP-7A40-83586). National Renewable Energy Lab.(NREL), Golden, CO (United States).
- [29] NingBo Deye Inverter Technology Co (2022) ‘mixroinverter’< https://www.deyeinverter.com/product/microinverter-1/?gclid=Cj0KCQjw1ZeUBhDyARIsAOzAqQixZ-M3tu9bF6YptiDqvoaXdZ3_k92ICFriyc7kIBVTTBGGAK5Jh4aAtUjEALw_wcB>
- [30] Chen Y. and Smedley K., (2008) ‘Three-phase boost-type grid-connected inverter,” IEEE Trans. Power Electron., vol. 23, DOI 10.1109/TPEL.2008.2003025, no. 5, pp. 2301–2309.
- [31] Chiu H.J. et al., (2010)‘A High Efficiency Dimmable LED Driver for Low-Power Lighting Applications”, IEEE Trans. Ind. Electron., vol. 57, no. 2, pp. 735–743.
- [32] Darwish A., Massoud A.M., Holliday D., Ahmed S., and Williams B.W.(2016)‘Single-Stage Three-Phase Differential-Mode Buck-Boost Inverters with Continuous Input Current for PV Applications’, in IEEE Transactions on Power Electronics, Vol.31, No.12, pp.8218–8236.
- [33] Rodriguez J. and Cortes P., (2012) ‘Predictive Control of Power Converters and Electrical Drives,’ John Wiley & Sons, vol. 40, 1st Edition, Chapter 1.
- [34] Elgbaily, M., Anayi, F., & Alshbib, M. M. (2022). A combined control scheme of direct torque control and field-oriented control algorithms for three-phase induction motor: Experimental validation. Mathematics, 10(20), 3842.
- [35] Gong, Z., Liu, C., Shang, L., Lai, Q., & Terriche, Y. (2022). Power decoupling strategy for voltage modulated direct power control of voltage source inverters connected to weak grids. IEEE Transactions on Sustainable Energy, 14(1), 152-167.